PSI Center for Nuclear Engineering and Sciences

Advancing Auger electron therapy: Developing methods for high-resolution spectral characterization of radioisotopes

Emilio A. Maugeri, Noemi Cerboni
Villigen, 3 September 2024

Measurement of branching and energies distribution of light charged particles during a radioactive decay

PSI

Table 1
Advanced list of the candidates for Targeted Auger Therapy.

Period	Radionuclide	$t_{½}$ Mother radionuclide	$t_{½}$ Daughter nuclide, years	Decay mode	Common energy X + γ, keV	Common energy β^- + Auger[4] + ce, keV	Common energy (Auger[4] + ce) <50 keV, keV	Number of e^-						Production method
								<0.15 keV	0.15–1.5 keV	1.5–10 keV	10–20 keV	20–50 keV	>50 keV	
I	II	III	IV	V	VI	VII	VIII	IX	X	XI	XII	XIII	XIV	XV
7	Bk-245	4.9 d	8500	EC, α	234	132	***16.8***	X	Y + Z	1.8	0.58	–	0.93	Accelerator
	Am-239	12 h	24,100	EC	239	168	***44.9***	X	Y + Z	3.6	0.89	0.58	0.95	Accelerator
	Pu-237	45 d	2,144,000	EC	52	16	***14.7***	X	Y + Z	1.4	0.41	0.36	0.2	Accelerator
	Np-239	2.4 d	24,100	β^-	173	260	***36.8***	X	Y + Z	2.3	0.5	0.52	1.80	Reactor, generator
	U-237	6.8 d	2,144,000	β^-	146	197	***40.2***	X	Y + Z	2.4	0.72	0.45	1.89	Reactor + ms, (generator)
	U-231	4.2 d	32,760	EC	82.1	71.1	***47.4***	X	Y + Z	2.9	0.86	0.65	0.38	Accelerator
	Th-231	26 h	32,760	β^-	25.7	165	***58.9***	X	Y + Z	2.8	1.2	0.75	1.46	Reactor + ms, (generator)
	Pa-229	1.5 d	7880	EC, α										Accelerator + ms
6	Tl-201	3 d	Stable	EC	93	43	***16.8***	X^1	Y^1	2.8	0.40	0.05	0.32	Accelerator
	Hg-197	64 h	Stable	EC	70	66	***13.4***	X^2	Y^2	2.6	0.39	–	0.80	Accelerator, reactor
	Pt-195m	4.3 d	Stable	IT	76	183	***51.6***	X^3	Y^3	4.5	0.77	0.87	1.23	Reactor, accelerator
	Pt-193m	4.0 d	50	IT	13	137	***21.8***	X^4	Y^4	3.8	0.42	–	1	Accelerator
	Ir-193m	10 d	Stable	IT										accelerator
	Ir-189	13 d	Stable[b]	EC	81	48	***21.9***	X	Y	2.8	0.07	0.30	0.31	Accelerator
	Os-191	15 d	Stable[b]	β^-	80	135	***82.8***	X	Y	3	0.05	***2***	0.76	Reactor + ms
	Os-189m	6 h	Stable	IT	2	29	***29***	X	Y	1.6	0.72	0.31	–	Generator
	Ta-180m	8.2 h	Stable	EC, β^-	48	55	***10.1***	X	Y	2.1	–	0.08	0.35	Accelerator
	Ta-177	57 h	Stable	EC	67	24	***11.9***	X	Y	2.2	–	0.08	0.12	Accelerator
	Lu-177	6.7 d	Stable	β^-	35	157	***9.5***	X	Y	0.3	–	0.17	0.98	Reactor
	Yb-169	32 d	Stable	EC	309	124	***34***	X	Y	6.7	0.11	0.19	0.99	Accelerator, reactor
	Tm-167	9.2 d	Stable[b]	EC	145	128	***20***	X	Y	3.4	–	0.2	0.62	Accelerator
	Er-165	10 h	Stable	EC	38	8	***8***	X	Y	2.0	–	0.05	–	Accelerator
	Ho-161	2.5 h	Stable	EC	61	33	***29.8***	X	Y	~3	0.51	0.37	0.05	Accelerator
	Tb-161	6.9 d	Stable	β^-	35	198	***29.3***	X	Y	~2	0.39	0.69	1.01	Reactor
	Tb-155	5.3 d	Stable	EC	138	32	***16.8***	X	Y	3.6	0.16	0.16	0.17	Accelerator
	La-135	19 h	Stable	EC, β^+	36	7	***6.9***	X^5	1.5	0.8	–	0.08	–	Accelerator
5	Cs-131	9.7 d	Stable	EC	23	7	***7***	X	1.5	0.8	–	0.09	–	Reactor
	I-125	60 d	Stable	EC	42	19	***19***	X^6	3	2.4	–	0.33	–	Reactor
	I-123	13 h	Stable	EC	171	28	***7.5***	X^7	1.8	1.0	–	0.12	0.16	Accelerator
	Te-125m	58 d	Stable	IT	36	109	***18.2***	X	2.9	2.4	–	0.29	0.97	Generator
	Sb-119	38 h	Stable	EC	23	26	***26***	X^8	2.8	1.5	0.68	0.28	–	Accelerator
	Sn-117m	14 d	Stable	IT	158	161	***6.7***	X	1.8	0.9	–	0.1	1.12	Accelerator
	In-111	2.8 d	Stable	EC	405	34	***7***	X^9	1.9	1.0	0.11	0.05	0.16	Accelerator
	Cd-107	6.5 h	Stable[b]	EC, β^+	34	87	***10.3***	X	3.2	1.7	0.15	0.07	0.95	Accelerator
	Pd-103	17 d	Stable[b]	EC	16	44	***44***	X	3.2	1.7	0.28	*0.91*	–	Accelerator
	Rh-103m	56 m	Stable	IT	2	38	***38***	X	1.5	0.8	0.12	***0.9***	–	Generator
	Tc-99m	6 h	211,100	IT	126	16	***2.8***	X	1.1	1.1	0.02	–	0.11	Generator
4	Ge-71	11 d	Stable	EC	4	5	***5***	2.5	1.2	0.42	0.01	–	–	Accelerator
	Ga-67	78 h	Stable	EC	158	36	***6.6***	3.5	1.7	0.61	–	–	0.33	Accelerator
	Co-60m	10 m	5.3	IT, β^-	7	58	***4.4***	2.8	1.37	0.60	–	–	0.98	Generator
	Co-58m	9.2 h	0.192	IT	2	23	***23***	2.7	1.3	0.46	0.75	0.25	–	Accelerator
	Cr-51	28 d	Stable	EC	33	4	***4***	3.2	1.5	0.68	–	–	0.00	Accelerator
3	Ar-37	35 d	Stable	EC	0.2	2.6	***2.6***	X	Y	0.83	–	–	–	Accelerator

Illustration of the tracks of α-particle, β-particle, and auger e- radiation

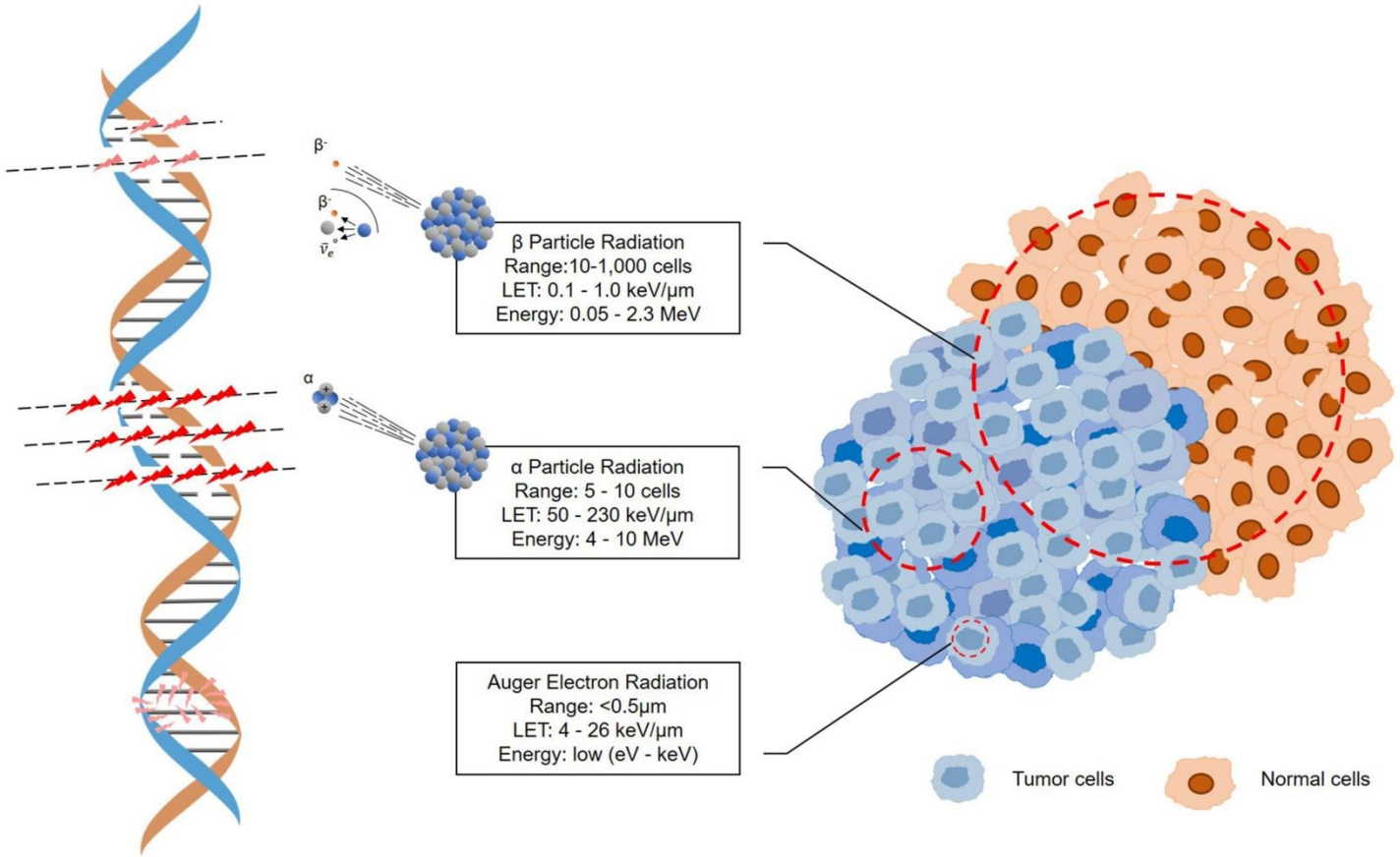

To effectively utilize Auger electrons in nuclear medicine, it is essential to have precise knowledge of their complete energy spectrum emitted per nuclear decay.

Shi M. et al. Alpha-peptide receptor radionuclide therapy using actinium-225 labeled somatostatin receptor agonists and antagonists. *Front Med*. 2022;9:1034315.

Measurement of branching and energies distribution of light charged particles during a radioactive decay

PSI

Table 1
Advanced list of the candidates for Targeted Auger Therapy.

Period	Radionuclide	$t_{½}$ Mother radionuclide	$t_{½}$ Daughter nuclide, years	Decay mode	Common energy X + γ, keV	Common energy β^- + Auger[a] + ce, keV	Common energy (Auger[a] + ce) <50 keV, keV	Number of e^-						Production method
								<0.15 keV	0.15–1.5 keV	1.5–10 keV	10–20 keV	20–50 keV	>50 keV	
I	II	III	IV	V	VI	VII	VIII	IX	X	XI	XII	XIII	XIV	XV
7	Bk-245	4.9 d	8500	EC, α	234	132	***16.8***	X	Y + Z	1.8	0.58	–	0.93	Accelerator
	Am-239	12 h	24,100	EC	239	168	***44.9***	X	Y + Z	3.6	0.89	0.58	0.95	Accelerator
	Pu-237	45 d	2,144,000	EC	52	16	***14.7***	X	Y + Z	1.4	0.41	0.36	0.2	Accelerator
	Np-239	2.4 d	24,100	β^-	173	260	***36.8***	X	Y + Z	2.3	0.5	0.52	1.80	Reactor, generator
	U-237	6.8 d	2,144,000	β^-	146	197	***40.2***	X	Y + Z	2.4	0.72	0.45	1.89	Reactor + ms, (generator)
	U-231	4.2 d	32,760	EC	82.1	71.1	***47.4***	X	Y + Z	2.9	0.86	0.65	0.38	Accelerator
	Th-231	26 h	32,760	β^-	25.7	165	***58.9***	X	Y + Z	2.8	1.2	0.75	1.46	Reactor + ms, (generator)
	Pa-229	1.5 d	7880	EC, α										Accelerator + ms
6	Tl-201	3 d	Stable	EC	93	43	***16.8***	X^1	Y^1	2.8	0.40	0.05	0.32	Accelerator
	Hg-197	64 h	Stable	EC	70	66	***13.4***	X^2	Y^2	2.6	0.39	–	0.80	Accelerator, reactor
	Pt-195m	4.3 d	Stable	IT	76	183	***51.6***	X^3	Y^3	4.5	0.77	0.87	1.23	Reactor, accelerator
	Pt-193m	4.0 d	50	IT	13	137	***21.8***	X^4	Y^4	3.8	0.42	–	1	Accelerator accelerator
	Ir-193m	10 d	Stable	IT										
	Ir-189	13 d	Stable[b]	EC	81	48	***21.9***	X	Y	2.8	0.07	0.30	0.31	Accelerator
	Os-191	15 d	Stable[b]	β^-	80	135	***82.8***	X	Y	3	0.05	***2***	0.76	Reactor + ms
	Os-189m	6 h	Stable	IT	2	29	***29***	X	Y	1.6	0.72	0.31	–	Generator
	Ta-180m	8.2 h	Stable	EC, β^-	48	55	***10.1***	X	Y	2.1	–	0.08	0.35	Accelerator
	Ta-177	57 h	Stable	EC	67	24	***11.9***	X	Y	2.2	–	0.08	0.12	Accelerator
	Lu-177	6.7 d	Stable	β^-	35	157	***9.5***	X	Y	0.3	–	0.17	0.98	Reactor
	Yb-169	32 d	Stable	EC	309	124	***34***	X	Y	6.7	0.11	0.19	0.99	Accelerator, reactor
	Tm-167	9.2 d	Stable[b]	EC	145	128	***20***	X	Y	3.4	–	0.2	0.62	Accelerator
	Er-165	10 h	Stable	EC	38	8	***8***	X	Y	2.0	–	0.05	–	Accelerator
	Ho-161	2.5 h	Stable	EC	61	33	***29.8***	X	Y	-3	0.51	0.37	0.05	Accelerator
	Tb-161	6.9 d	Stable	β^-	35	198	***29.3***	X	Y	-2	0.39	0.69	1.01	Reactor
	Tb-155	5.3 d	Stable	EC	138	32	***16.8***	X	Y	3.6	0.16	0.16	0.17	Accelerator
	La-135	19 h	Stable	EC, β^+	36	7	***6.9***	X^5	1.5	0.8	–	0.08	–	Accelerator
5	Cs-131	9.7 d	Stable	EC	23	7	***7***	X	1.5	0.8	–	0.09	–	Reactor
	I-125	60 d	Stable	EC	42	19	***19***	X^6	3	2.4	–	0.33	–	Reactor
	I-123	13 h	Stable	EC	171	28	***7.5***	X^7	1.8	1.0	–	0.12	0.16	Accelerator
	Te-125m	58 d	Stable	IT	36	109	***18.2***	X	2.9	2.4	–	0.29	0.97	Generator
	Sb-119	38 h	Stable	EC	23	26	***26***	X^8	2.8	1.5	0.68	0.28	–	Accelerator
	Sn-117m	14 d	Stable	IT	158	161	***6.7***	X	1.8	0.9	–	0.1	1.12	Accelerator
	In-111	2.8 d	Stable	EC	405	34	***7***	X^9	1.9	1.0	0.11	0.05	0.16	Accelerator
	Cd-107	6.5 h	Stable[b]	EC, β^+	34	87	***10.3***	X	3.2	1.7	0.15	0.07	0.95	Accelerator
	Pd-103	17 d	Stable[b]	EC	16	44	***44***	X	3.2	1.7	0.28	*0.91*	–	Accelerator

The problem is most effectively addressed using Monte Carlo simulations based on decay rates calculated for isolated atoms. It is then highly desirable to experimentally verify these results, specifically the predicted number of Auger electrons produced per nuclear decay and their energies.

Very few experimental data so far

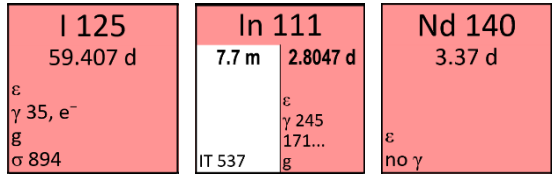

Accurately determining the number of e⁻ Auger e per nuclear decay for ^{125}I

IOP Publishing Phys. Med. Biol. 63 (2018) 06NT04 (6pp) https://doi.org/10.1088/1361-6560/aab24b

Physics in Medicine & Biology

IPEM Institute of Physics and Engineering in Medicine

CrossMark

NOTE

Measurement of the intensity ratio of Auger and conversion electrons for the electron capture decay of ^{125}I

RECEIVED
11 October 2017

REVISED
23 February 2018

ACCEPTED FOR PUBLICATION
26 February 2018

PUBLISHED
21 March 2018

M Alotiby[1,2], I Greguric[3], T Kibédi[4], B Q Lee[4,5], M Roberts[3], A E Stuchbery[4], Pi Tee[4], T Tornyi[4,6] and M Vos[1]

[1] Electronic Materials Engineering, Research School of Physics and Engineering, Australian National University, Canberra ACT, Australia
[2] King Abdulaziz City for Science and Technology, Riyadh, Saudi Arabia
[3] Australian Nuclear Science and Technology Organisation, Lucas Heights, NSW, Australia
[4] Nuclear Physics, Research School of Physics and Engineering, Australian National University, Canberra, ACT, Australia
[5] Present address: Department of Oncology, Oxford University, Oxford, United Kingdom
[6] Present address: ATOMKI, Debrecen, Hungary

E-mail: maarten.vos@anu.edu.au and tibor.kibedi@anu.edu.au

Keywords: ^{125}I, Auger intensity, conversion electron intensity

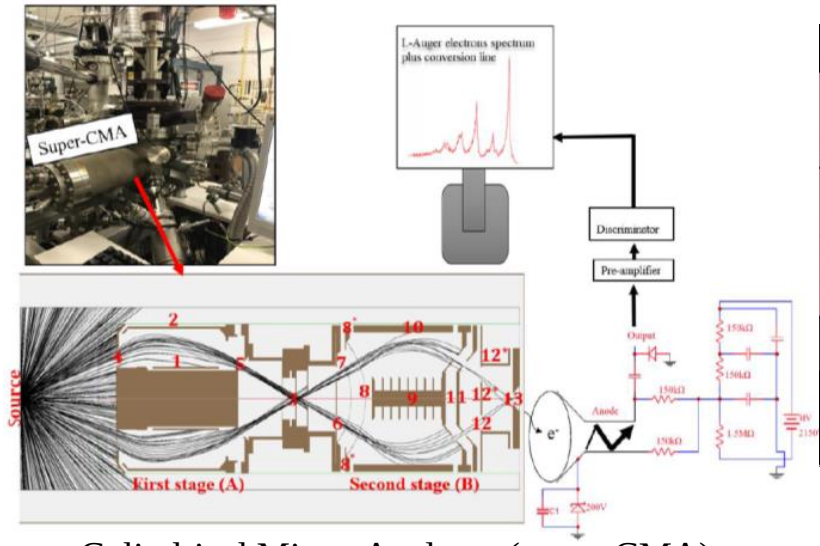

Cylindrical Mirror Analyser (super-CMA)

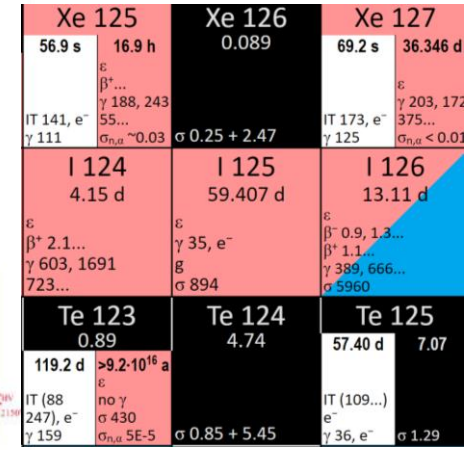

The measurements were performed with two spectrometers. For 50 eV to 4 keV (LMM Auger and K CE), the DESA100 SuperCMA (Staib Instruments) was used. An Electron Momentum Spectrometer was used for higher energies, up to 40 keV

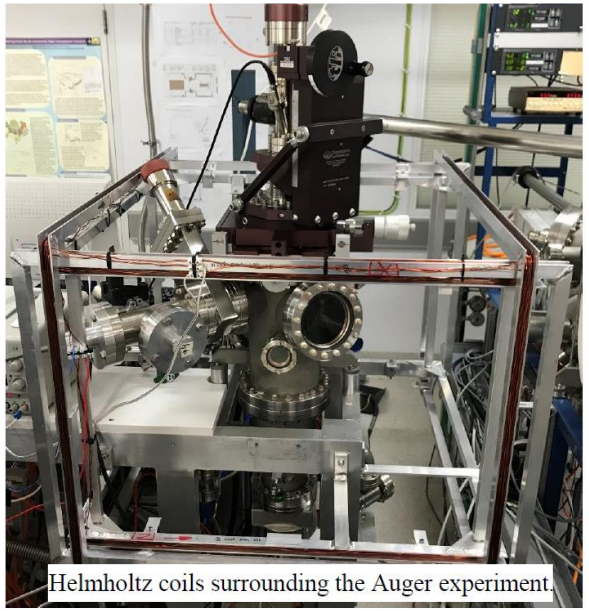

Helmholtz coils surrounding the Auger experiment.

Accurately determining the number of e⁻ Auger e per nuclear decay for ^{125}I

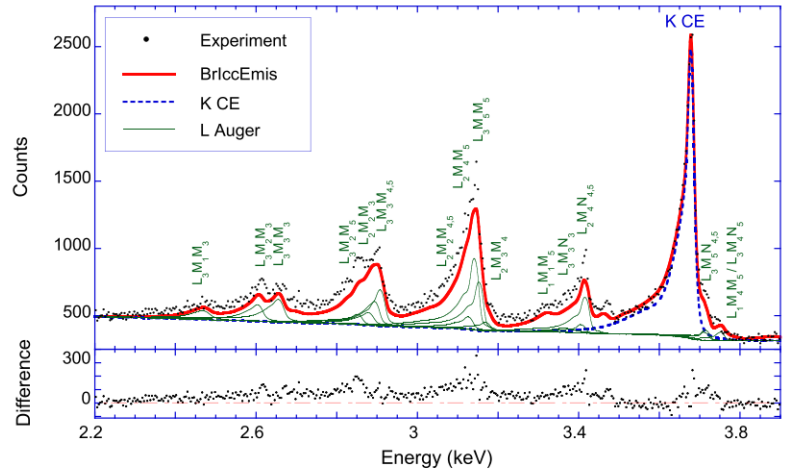

Figure 2. The measured spectrum (dots) of the K-CE and LMM Auger electrons. The solid red line is the calculated spectrum based on BrIccEmis scaled to the K-CE line. The contribution of the conversion electrons (blue, dashed line) and the strongest individual Auger electron contributions (thin green lines) are indicated as well. The lower panel shows the residual of the fit and the non-zero difference indicate that the theory underestimates the Auger intensity, relative to the CE intensity.

Phys. Med. Biol. **63** (2018) 06NT04 (6pp) M Alotiby *et al*

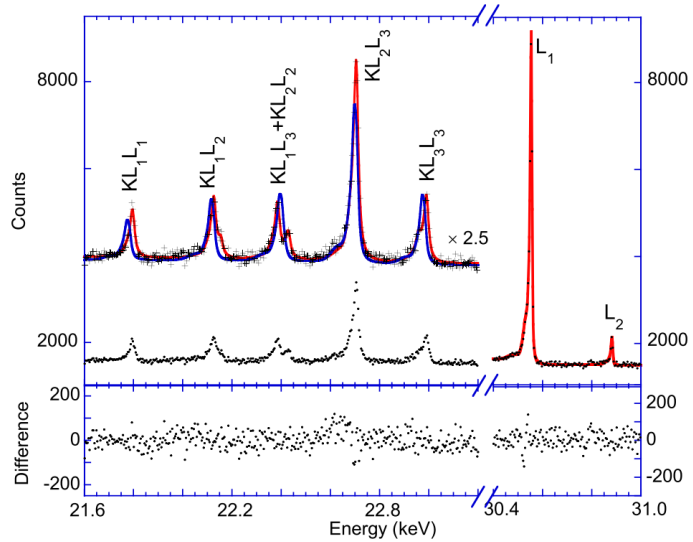

Figure 1. The KLL Auger and L_1, L_2-CE spectrum as measured in a single run. The red line shows a fit of the KLL spectrum with eight peaks following the approach of Larkins (1977) (residuals in lower panel). The blue line shows a description of the KLL spectrum based on the BrIccEmis calculation (Lee *et al* 2016) which was scaled such that the calculated L_1 CE line has the same area as the measured one. The calculated Auger spectrum, normalised in this way, has an area that is smaller than the observed one.

4. Conclusion and discussion

The combined K CE—LMM Auger measurement indicates that the experimental relative Auger intensity is about 15-20% higher than the calculated one. The same order of magnitude of difference was found for the KLL Auger intensity compared to the L_1-CE intensity, in spite of the fact that the energies involved were rather different and that two different spectrometers were used.

Challenges in Obtaining Auger Electron Experimental Spectra

PSI

Preparation of the e⁻ Auger source

Production of the e⁻ Auger radionuclide

Measurement and interpretation of the resulting spectra

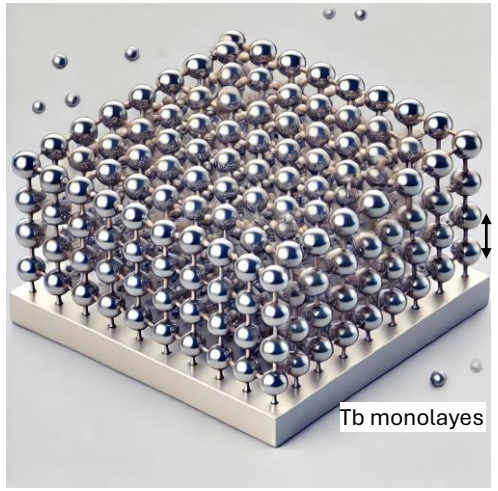

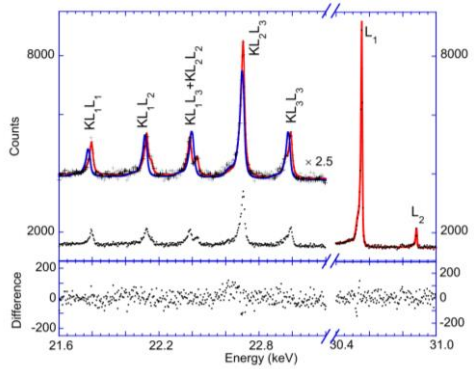

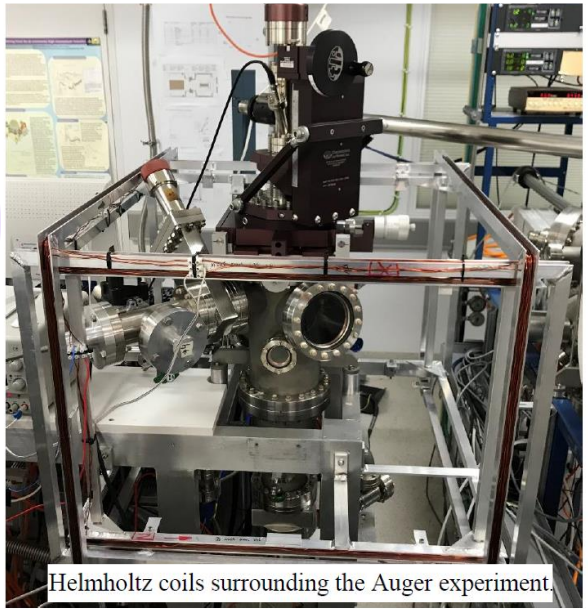
Helmholtz coils surrounding the Auger experiment.

Challenges in Obtaining Auger Electron Experimental Spectra

PSI

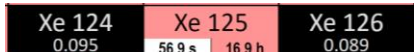

Applied Radiation and Isotopes 211 (2024) 111405

Contents lists available at ScienceDirect

Applied Radiation and Isotopes

journal homepage: www.elsevier.com/locate/apradiso

Low-energy Auger and conversion electron spectroscopy of ^{99}Mo β^--decay

B.P.E. Tee [a,*], M.P. Roberts [b], Paul A. Pellegrini [b], Flora Mansour [b], Leena Burgess [b], M. Vos [c], T. Kibédi [a]

[a] Department of Nuclear Physics and Accelerator Applications, Australian National University, Canberra, Australia
[b] Australian Nuclear Science and Technology Organisation (ANSTO), Lucas Heights, Australia
[c] Department of Materials Physics, Research School of Physics, Australian National University, Canberra, Australia

ANSTO

Preparation of the ^{125}I source (4 mm diameter with an activity of 6 MBq)

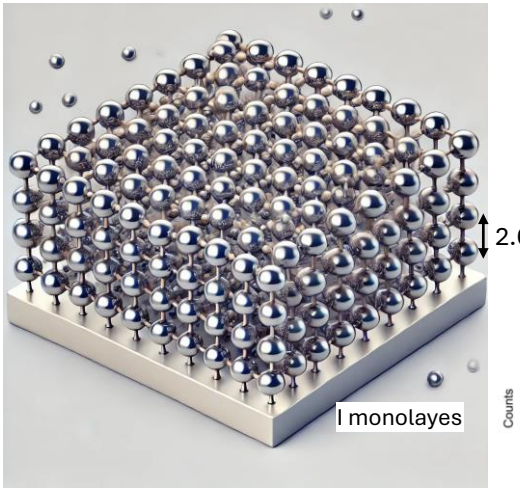

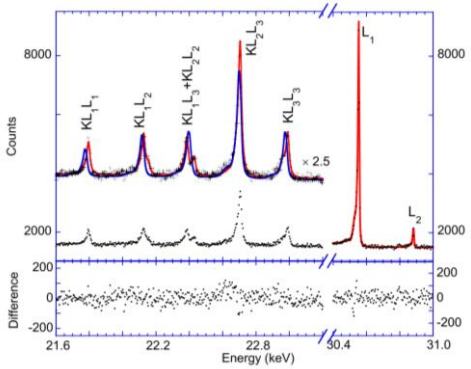

Production of the ^{125}I

Measurement and interpretation of the resulting spectra

ANSTO (Australian Nuclear Science and Technology Organisation)

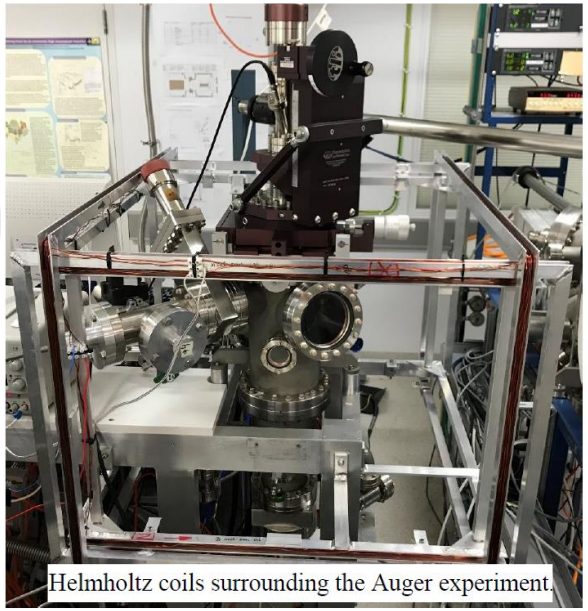

Australian National University, Canberra

Challenges in Obtaining Auger Electron Experimental Spectra

PSI

Isotope and Target Chemistry Group

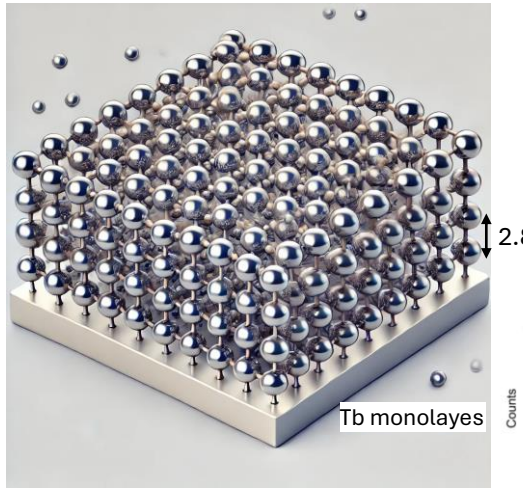

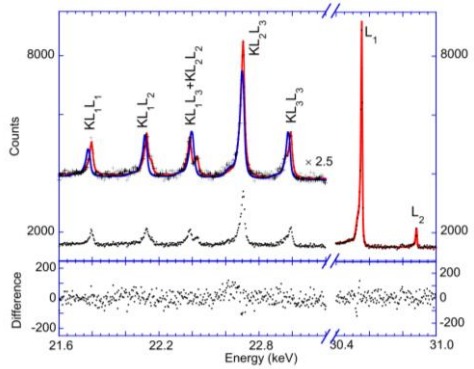

PSI proton accelerator

SINQ – Swiss Spallation Neutron Source (ILL High-Flux Reactor, CERN's MEDICIS facility)

Preparation of the e⁻ Auger source

Production of the e⁻ Auger radionuclide

Measurement and interpretation of the resulting spectra

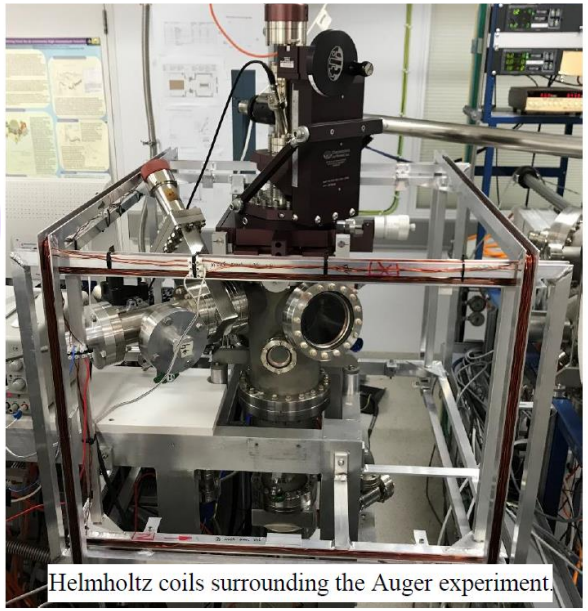

Preparation of Lanthanides e^- Auger emitting radionuclides sources

La 135	Pr 149	Sm 153	Tb 155	Tb 161	Ho 161		Er 165	Tm 167	Yb 169		Lu 177		
19.4 h	2.25 m	46.284 h	5.32 d	6.89 d	6.76 s	2.48 h	10.36 h	9.25 d	46 s	32.018 d	7 m	160.44 d	6.647 d
ε, β^+... γ 481, (875 588...) g	β^- 3.0... γ 138, 165 109...	β^- 0.7, 0.8... γ 103, 70..., e^- σ 420	ε γ 87, 105, 180 262...	β^- 0.5, 0.6... γ 26, 49, 75... e^-	IT 211, e^-	ε γ 26, 103 78..., e^-	ε no γ	ε γ 532... m	IT (24) e^-	ε γ 63 198, 177 110... σ 3600	β^- γ 1003 89... m_2	β^- 0.2 m_1 IT (116) e^-, γ 414 319... σ 3.2	β^- 0.5... γ 208 113... g σ 1000

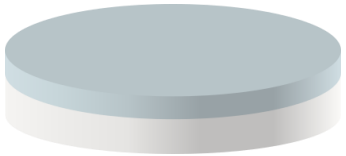

- Sources must be **mechanically stable.**
- e^- should have the same probability of interaction with the source nuclei. Thus, sources must be **homogeneous** and have **uniform thickness**.
- Must be **thin enough** (few nm) to let e^- pass through.
- The production method must have **high yields**, almost quantitative, due to the cost of the source material and be reasonably fast due to the short $t_{1/2}$ of the radionuclides.
- The ideal source is a monolayer of a radionuclide in its elemental state.
- Lanthanides are typically metals, so their "elemental state" would refer to their pure metallic form.

Methods for Preparation of Lns e⁻ Auger emitting radionuclides sources

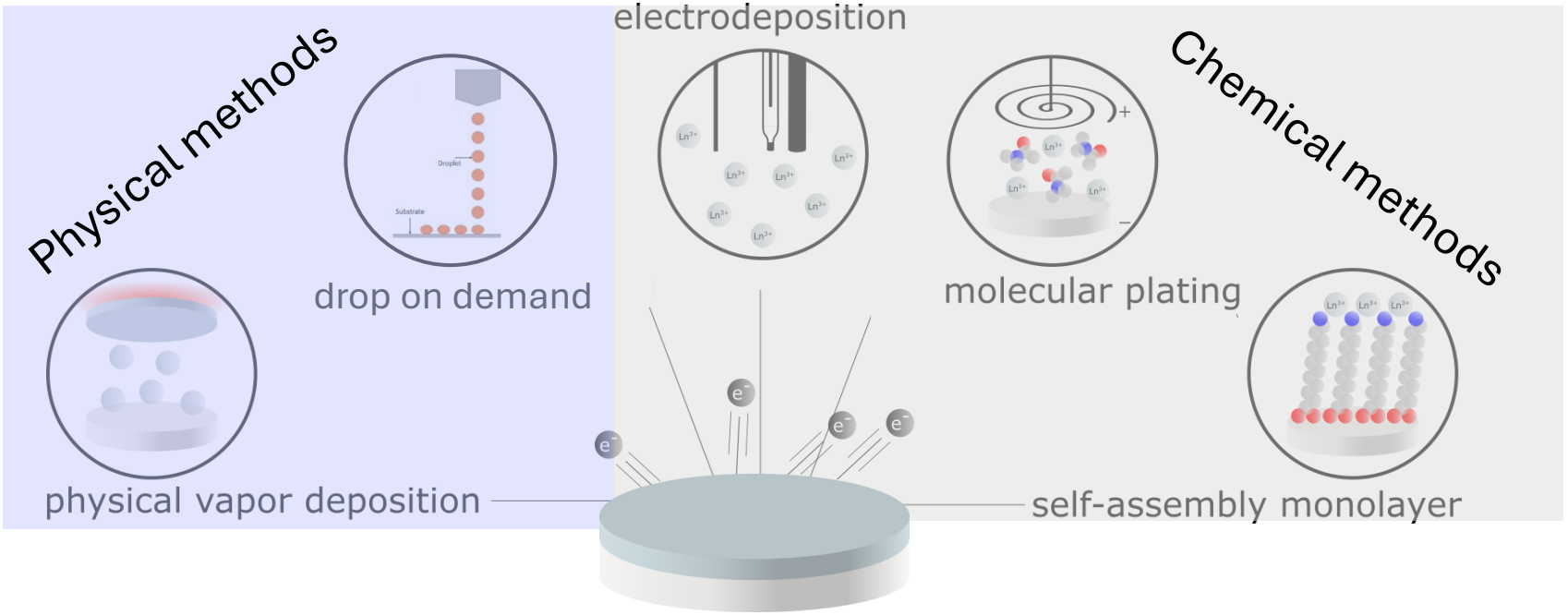

Methods for Preparation of Lns e⁻ Auger emitting radionuclides sources

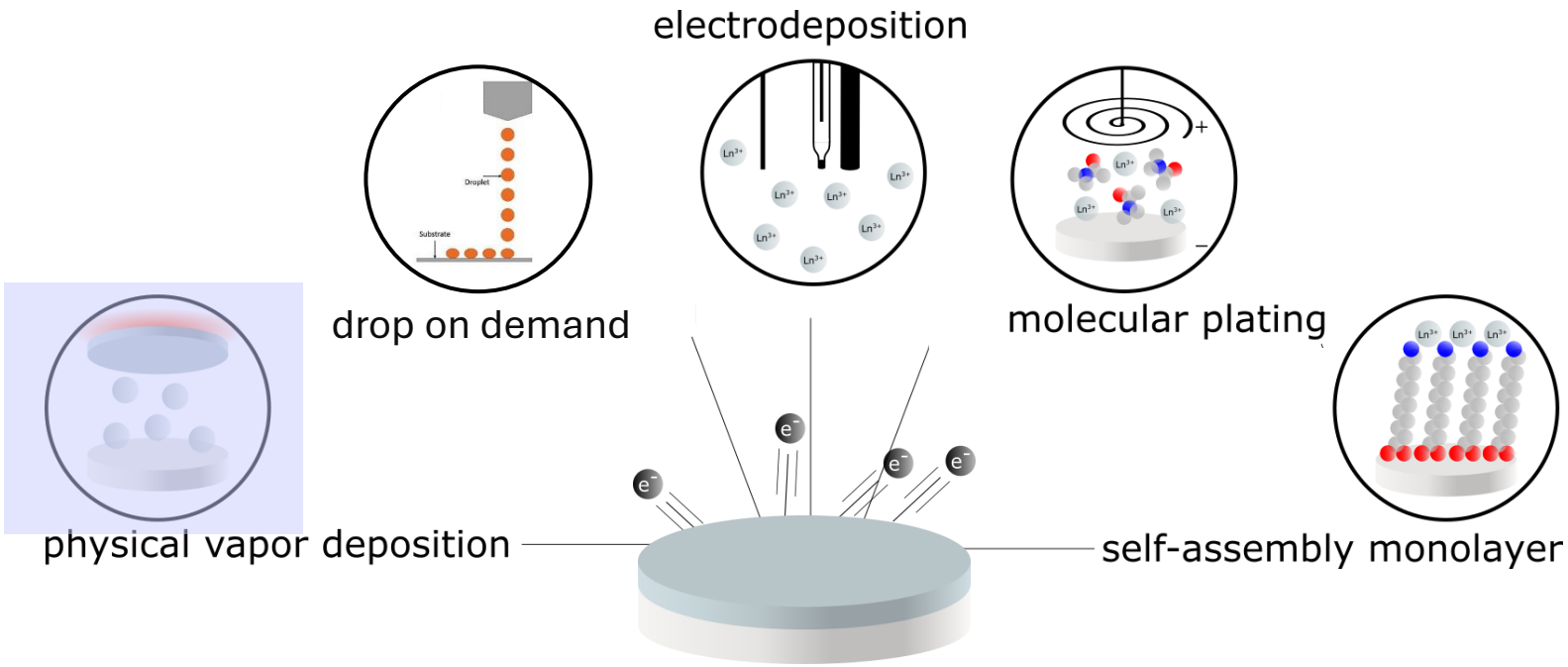

Physical Phase Deposition

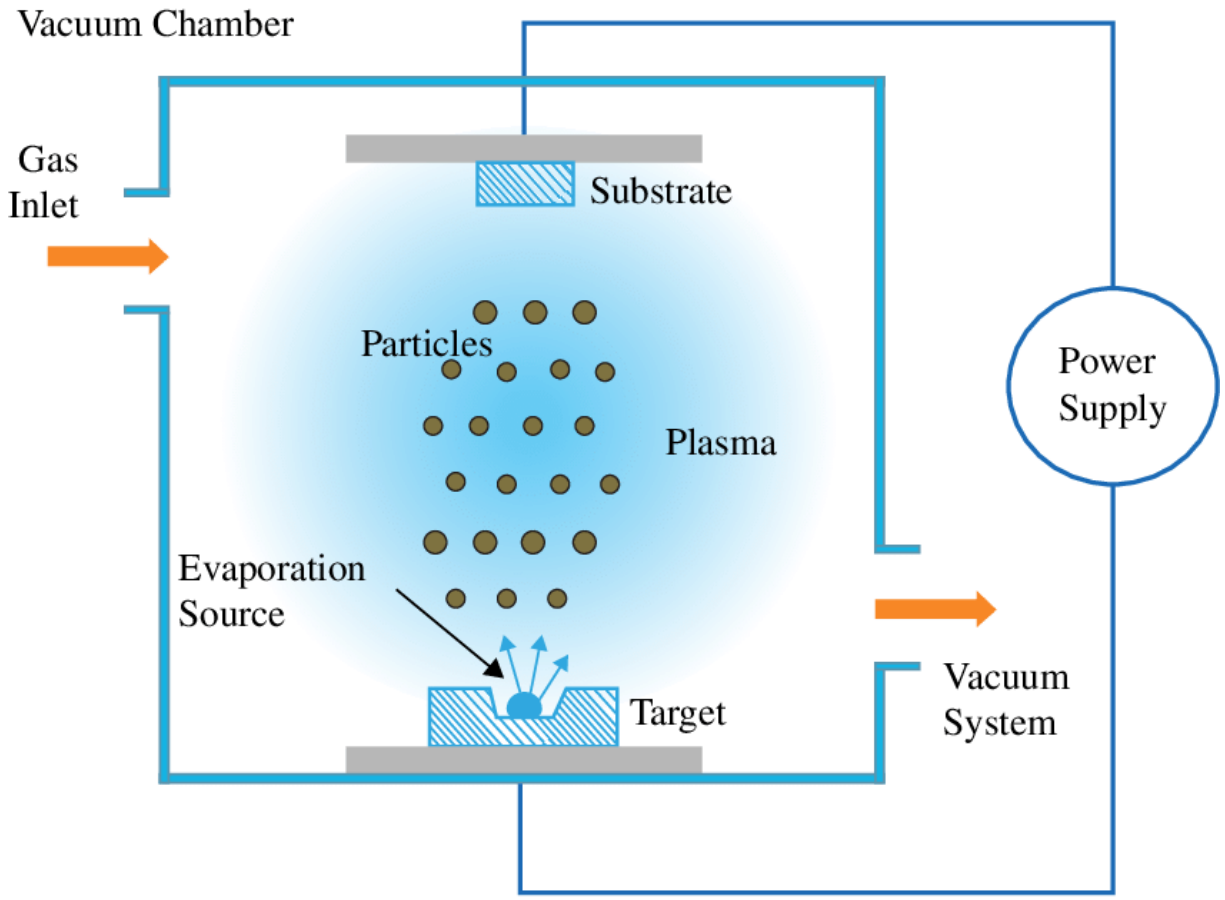

- Uniform depositions
- Thin layers
- Low Yields (less than 30%)
- Radioprotection issues

Methods for Preparation of Lns e⁻ Auger emitting radionuclides sources

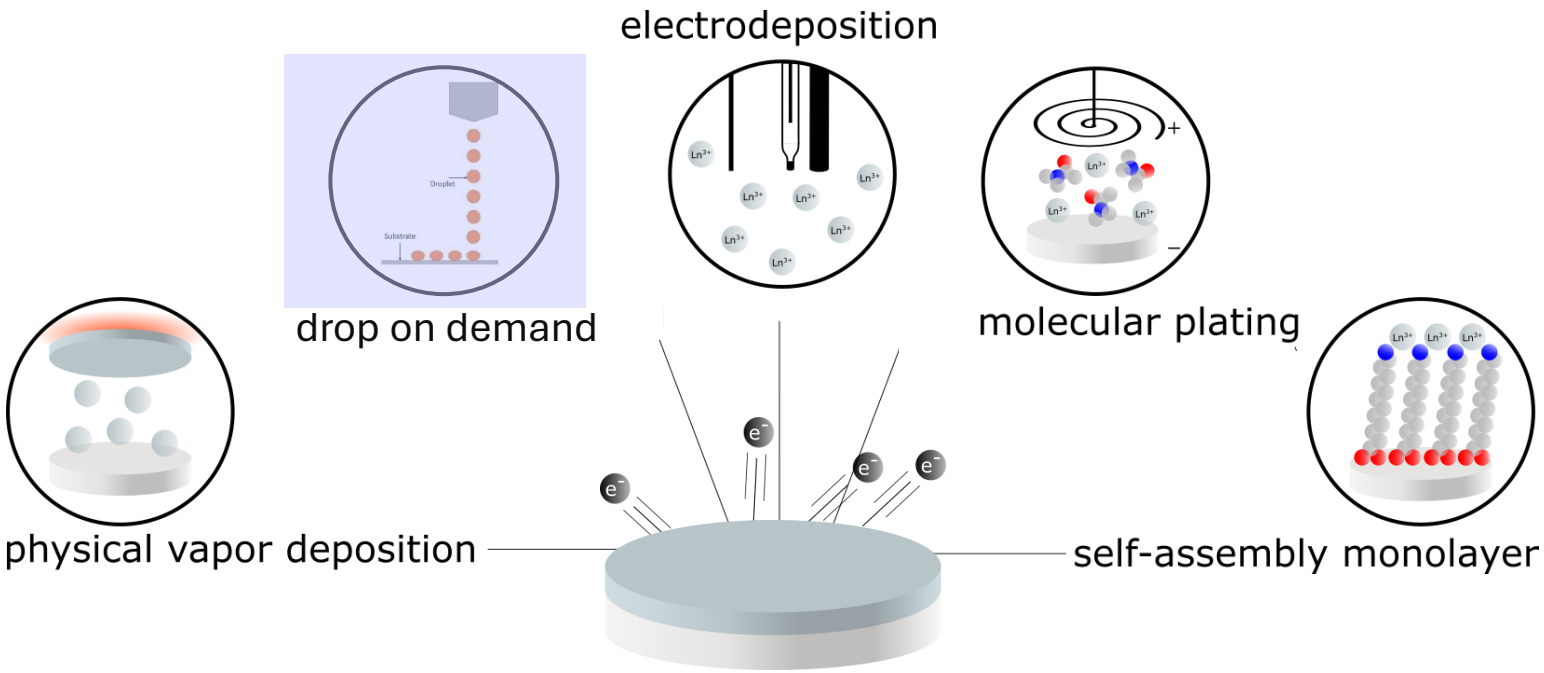

Drop on demand

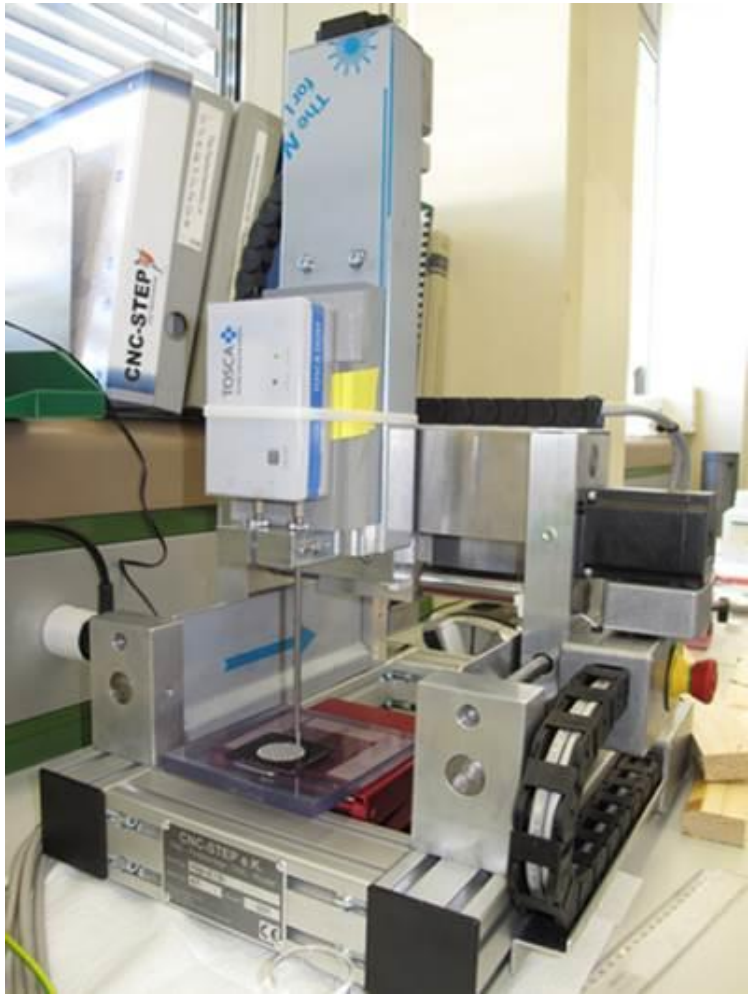

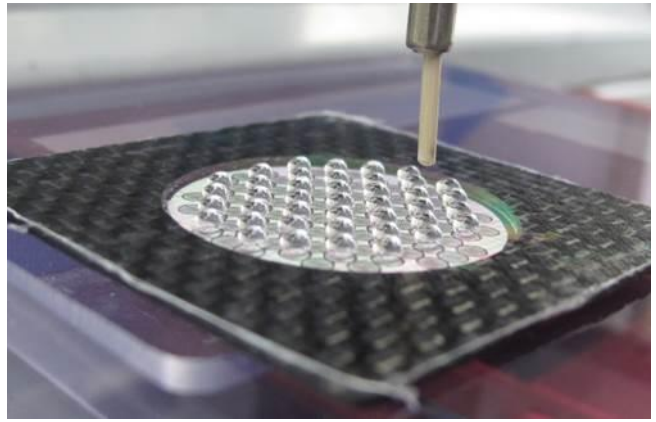

- High Yields (about 100%)
- Not uniform
- Thick layer

Electroplating from aqueous and non aqueous solution

Standard Reduction Potentials in Aqueous Solutions at 25 °C

Oxidizing Agent				Reducing Agent	Reduction Potential (V)
F_2	+	$2e^-$	→	$2F^-$	2.87
H_2O_2	+	$2H^+ + 2e^-$	→	$2H_2O$	1.78
MnO_4^-	+	$8H^+ + 5e^-$	→	$Mn^{2+} + 4H_2O$	1.51
Au^{3+}	+	$3e^-$	→	Au	1.50
Cl_2	+	$2e^-$	→	$2Cl^-$	1.36
O_2	+	$4H^+ + 4e^-$	→	$2H_2O$	1.23
$Cr_2O_7^{2-}$	+	$14H^+ + 6e^-$	→	$2Cr^{3+} + 7H_2O$	1.23
Br_2	+	$2e^-$	→	$2Br^-$	1.07
NO_3^-	+	$4H^+ + 3e^-$	→	$NO + 2H_2O$	0.96
Ag^+	+	e^-	→	Ag	0.80
I_2	+	$2e^-$	→	$2I^-$	0.54
Cu^+	+	e^-	→	Cu	0.52
O_2	+	$2H_2O + 4e^-$	→	$4OH^-$	0.40
Cu^{2+}	+	$2e^-$	→	Cu	0.34
$2H_3O^+$	+	$2e^-$	→	$H_2 + 2H_2O$	0.00
Pb^{2+}	+	$2e^-$	→	Pb	−0.13
Sn^{2+}	+	$2e^-$	→	Sn	−0.14
Ni^{2+}	+	$2e^-$	→	Ni	−0.26
Fe^{2+}	+	$2e^-$	→	Fe	−0.45
Cr^{3+}	+	$3e^-$	→	Cr	−0.74
Zn^{2+}	+	$2e^-$	→	Zn	−0.76
$2H_2O$	+	$2e^-$	→	$H_2 + 2OH^-$	−0.83
Mn^{2+}	+	$2e^-$	→	Mn	−1.19
Al^{3+}	+	$3e^-$	→	Al	−1.66
Mg^{2+}	+	$2e^-$	→	Mg	−2.37
Na^+	+	e^-	→	Na	−2.71
Ca^{2+}	+	$2e^-$	→	Ca	−2.87
Ba^{2+}	+	$2e^-$	→	Ba	−2.91
K^+	+	e^-	→	K	−2.93
Li^+	+	e^-	→	Li	−3.04

Increasing Strength of Oxidizing Agent ↑

Increasing Strength of Reducing Agent ↓

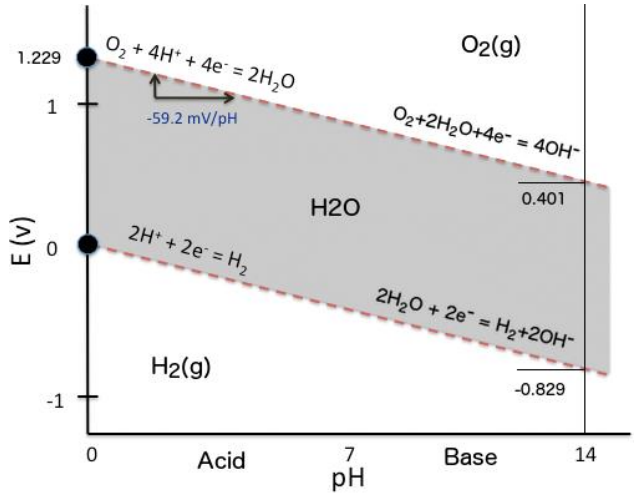

Pourbaix diagram for water

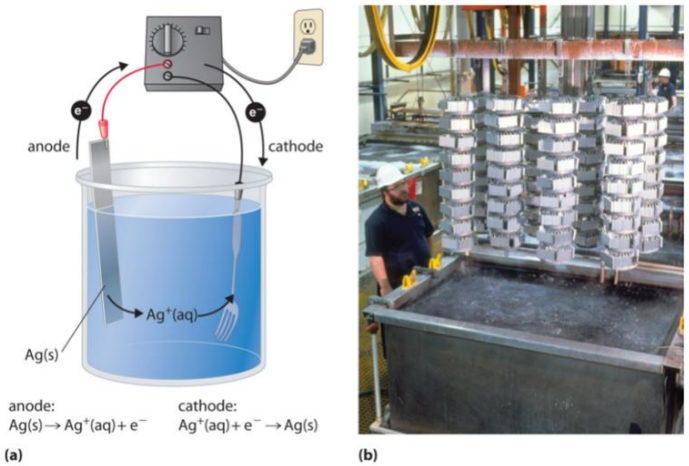

Figure 17.7.3: Electroplating. (a) Electroplating uses an electrolytic cell in which the object to be plated, such as a fork, is immersed in a solution of the metal to be deposited. The object being plated acts as the cathode, on which the desired metal is deposited in a thin layer, while the anode usually consists of the metal that is being deposited (in this case, silver) that maintains the solution concentration as it dissolves. (b) In this commercial electroplating apparatus, a large number of objects can be plated simultaneously by lowering the rack into the Ag^+ solution and applying the correct potential. (CC BY-SA-NC; anonymous)

Electrodeposition from IL

Standard Cathode (Reduction) Half-Reaction	Standard Reduction Potential E° (volts)
$Li^+(aq) + e^- \rightleftharpoons Li(s)$	-3.040
$Rb^+ + e^- \rightleftharpoons Rb\ (s)$	-2.98
$K^+(aq) + e^- \rightleftharpoons K(s)$	-2.93
$Ba^{2+} + 2e^- \rightleftharpoons Ba(s)$	-2.92
$Cs^+(aq) + e^- \rightleftharpoons Cs(s)$	-2.92
$Ba^{2+}(aq) + 2e^- \rightleftharpoons Ba(s)$	-2.91
$Sr^{2+}(aq) + 2e^- \rightleftharpoons Sr(s)$	-2.89
$Ca^{2+}(aq) + 2e^- \rightleftharpoons Ca(s)$	-2.84
$Na^+(aq) + e^- \rightleftharpoons Na(s)$	-2.713
$Mg(OH)_2(s) + 2e^- \rightleftharpoons Mg(s) + 2OH^-$	-2.687
$La^{3+} + 3e^- \rightleftharpoons La(s)$	-2.38
$Mg^{2+}(aq) + 2e^- \rightleftharpoons Mg(s)$	-2.356
$Ce^{3+} + 3e^- \rightleftharpoons Ce(s)$	-2.336
$Al(OH)_4^- + 3e^- \rightleftharpoons Al(s) + 4OH^-$	-2.310
$AlF_6^{3-} + 3e^- \rightleftharpoons Al(s) + 6F^-$	-2.07
$Be^{2+} + 2e^- \rightleftharpoons Be(s)$	-1.99
$B(OH)_4^- + 3e^- \rightleftharpoons B(s) + 4OH^-$	-1.811
$Al^{3+}(aq) + 3e^- \rightleftharpoons Al(s)$	-1.676
$U^{3+} + 3e^- \rightleftharpoons U(s)$	-1.66
$ZnO_2 + 4H^+ + 4e^- \rightleftharpoons Zr(s) + 2H_2O$	-1.473
$SiF_6^{2-} + 4e^- \rightleftharpoons Si(s) + 6F^-$	-1.37
$Zn(CN)_4^{2-} + 2e^- \rightleftharpoons Zn(s) + 4CN$	-1.34
$Zn(OH)_4^{2-} + 2e^- \rightleftharpoons Zn(s) + 4OH^-$	-1.285
$Mn^{2+} + 2e^- \rightleftharpoons Mn(s)$	-1.17

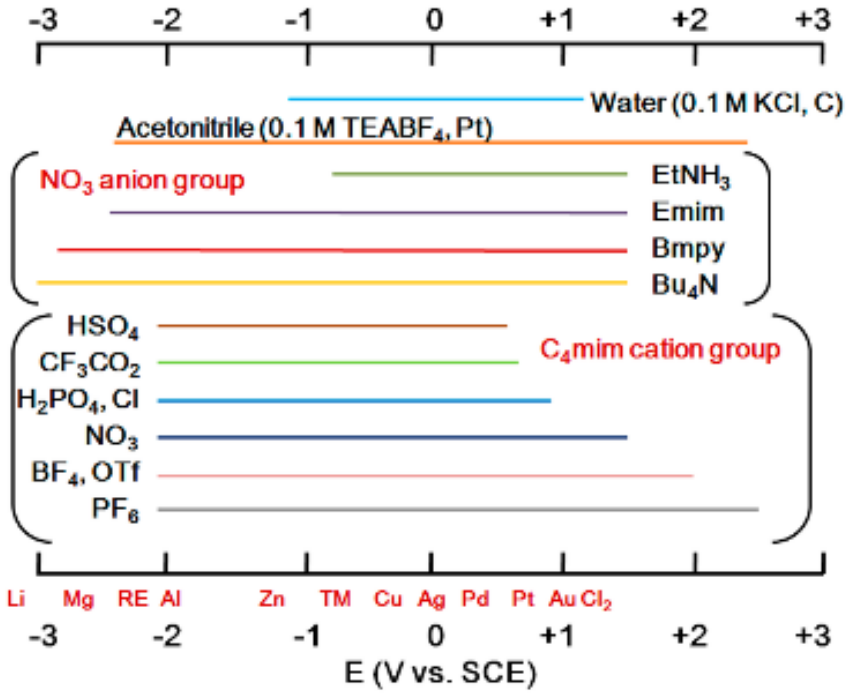

J. Park et al., 2014

For all lanthanides the reduction potentials are almost the same, ranging from −1.09 (for Nb) to −2.35 V (for Pr)

See poster of Noemi Cerboni

Molecular plating (MP) technique

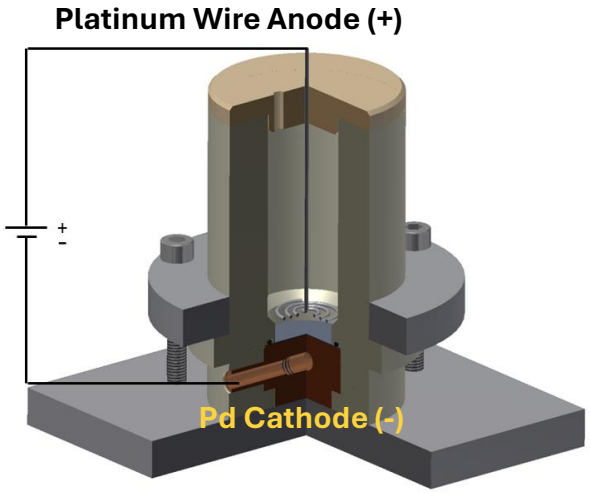

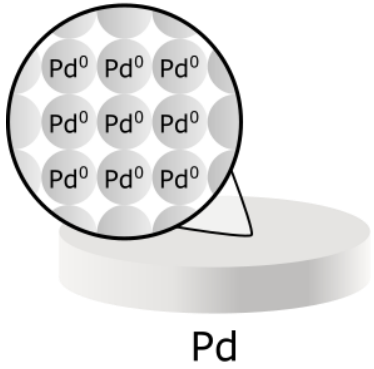

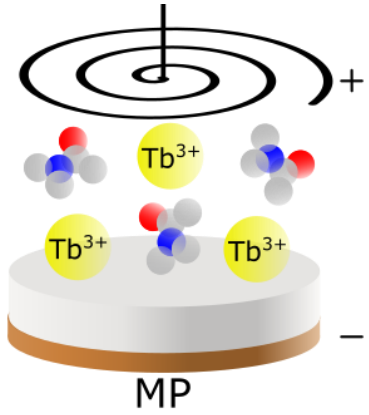

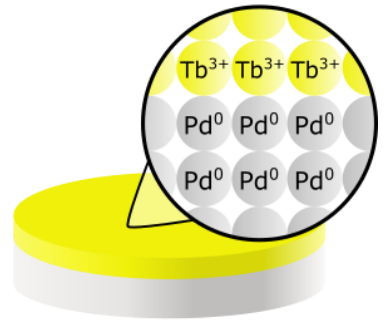

$$2\ H_2O + 2e^- \rightarrow H_2 + 2\ OH^-$$

$$3\ OH^- + Ln^{3+} \rightarrow Ln(OH)_3 \downarrow$$

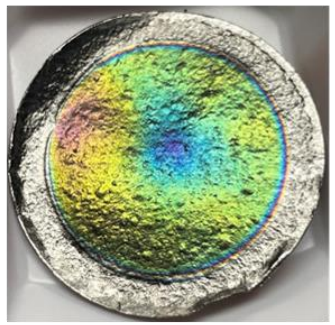

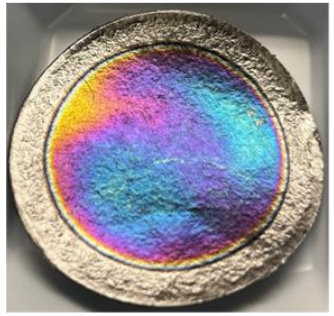

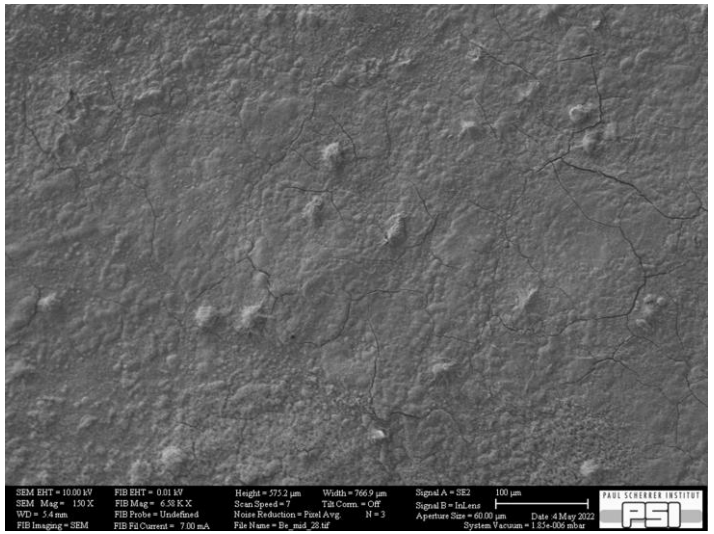

- High Yields (90/98%)
- Almost uniform layer
- Thickening of the deposit layer due to co-precipitation of other compounds

Coupled reduction (CR) technique

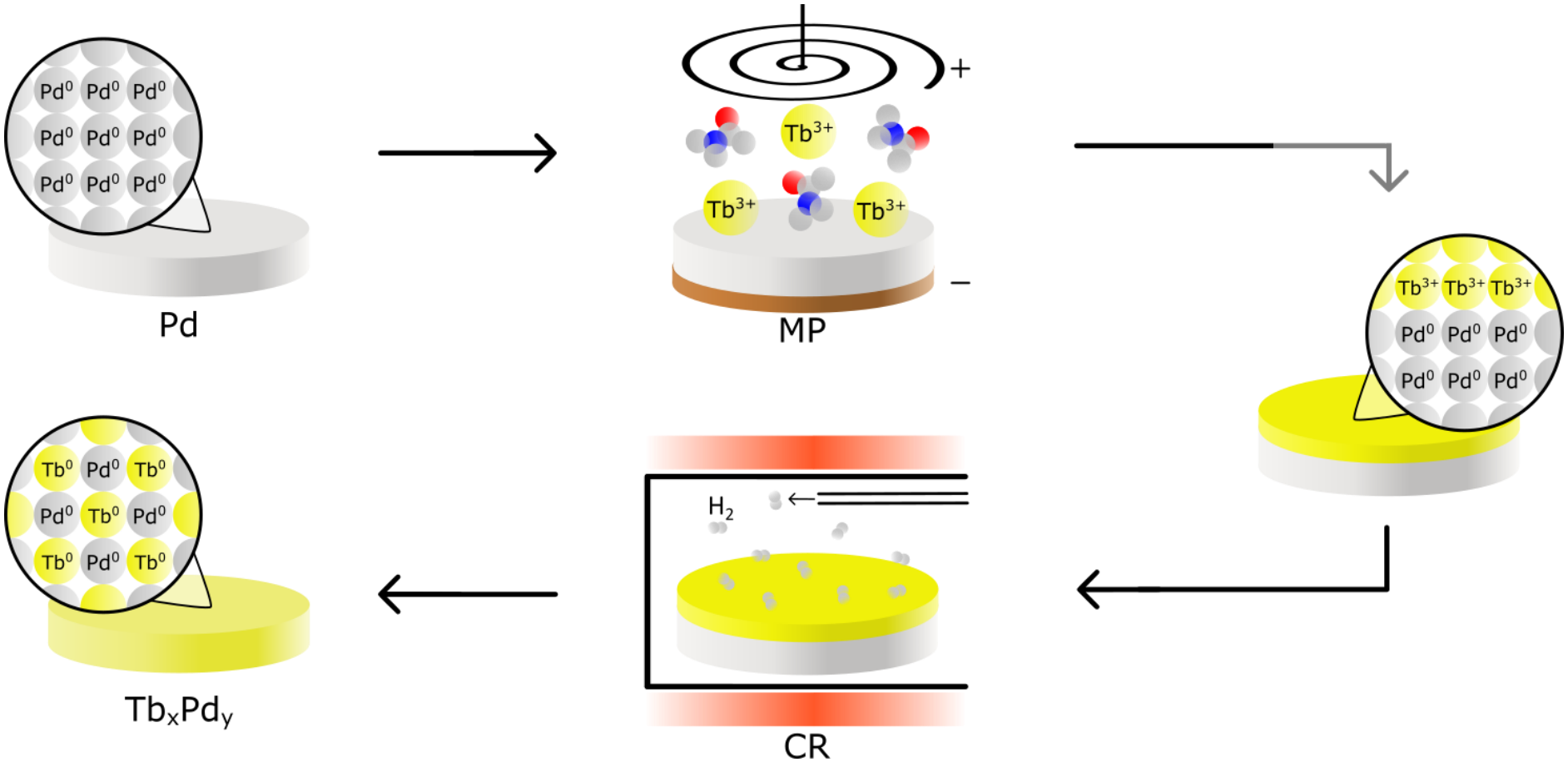

$$x\,Pd + Ln_yO_z + z\,H_2 \rightarrow Ln_yPd_x + z\,H_2O$$

Self-assembled monolayers (SAMs)

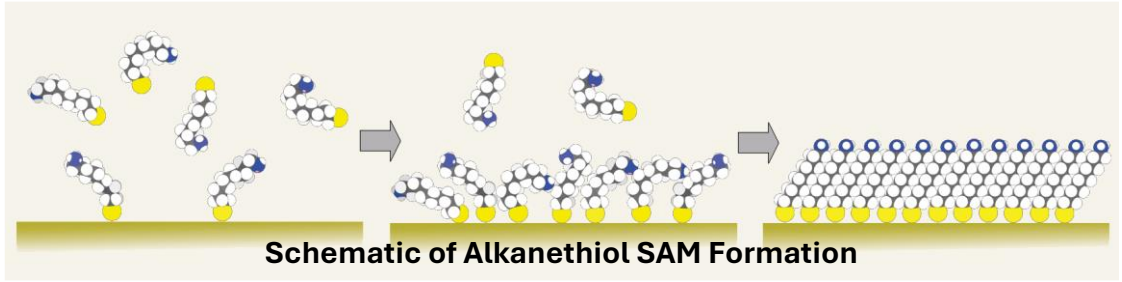

Schematic of Alkanethiol SAM Formation

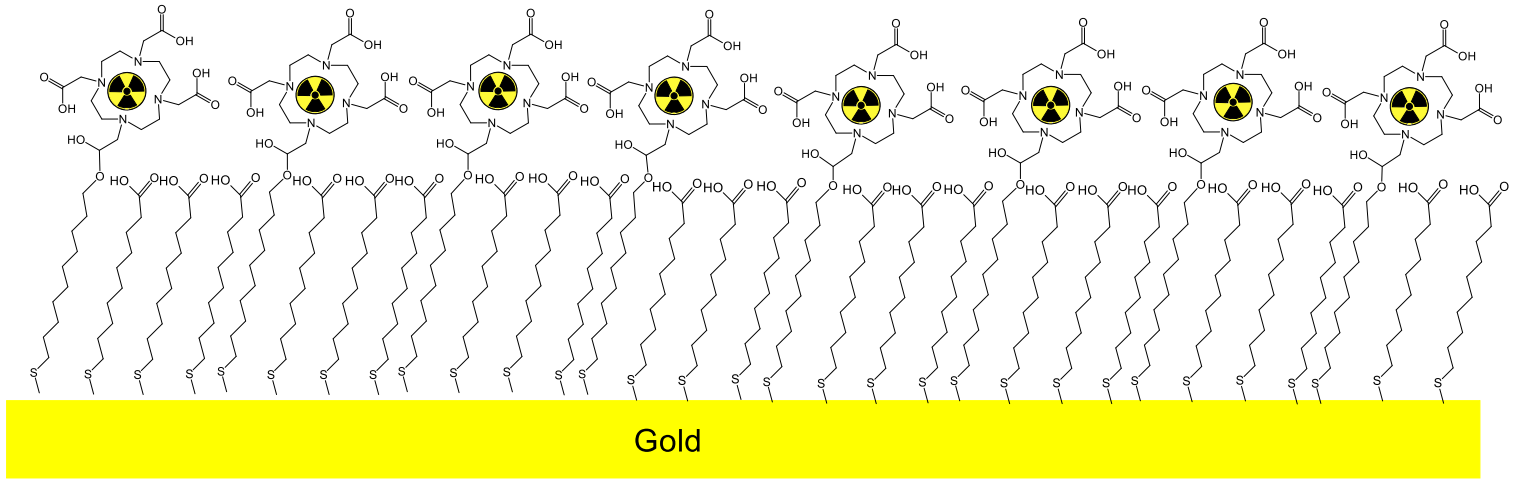

- High Yields Almost uniform layer
- Monolayer
- Homogeneous

Many Thanks!

Ionic liquid

Proposed method: production of thin, homogenous, and uniform targets via electrodeposition of micrograms or even nanograms of exotic radionuclides from ionic liquid electrolytes

Is a salt in the liquid state. At least one ion has a delocalized charge and one component is organic which prevents the formation of a stable crystal lattice

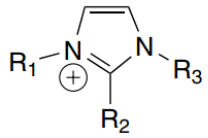

imidazolium

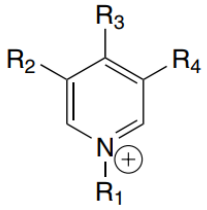

pyridinium

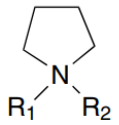

pyrrolidinium

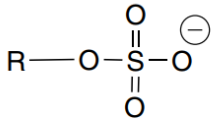

alkylsulfate

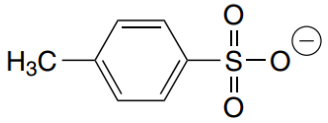

tosylate

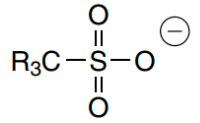

methanesulfonate

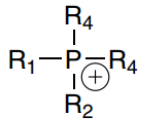

phosphonium

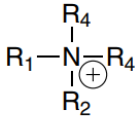

ammonium

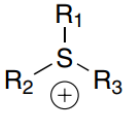

sulfonium

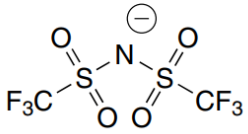

bis(trifluoromethyl-sulfonyl)imide

hexafluoro-phosphate

tetrafluoro-borate

halide

Cations commonly found in ionic liquids.

Anions.